Msi RNA-binding proteins control reserve intestinal stem cell quiescence

Maryam Yousefi,[1,3] Ning Li,[1] Angela Nakauka-Ddamba,[1] Shan Wang,[1,6] Kimberly Davidow,[1] Jenna Schoenberger,[1] Zhengquan Yu,[6] Shane T. Jensen,[5] Michael G. Kharas,[7] and Christopher J. Lengner[1,2,3,4]

[1]Department of Biomedical Sciences, School of Veterinary Medicine, [2]Department of Cell and Developmental Biology, School of Medicine, [3]Cell and Molecular Biology Graduate Program, [4]Institute for Regenerative Medicine, and [5]Department of Biostatistics, the Wharton School, University of Pennsylvania, Philadelphia, PA 19104
[6]State Key Laboratories for Agrobiotechnology, College of Biological Sciences, China Agricultural University, Beijing 100083, China
[7]Molecular Pharmacology and Chemistry Program, Experimental Therapeutics Center and Center for Stem Cell Biology, Memorial Sloan-Kettering Cancer Center, New York, NY 10065

Regeneration of the intestinal epithelium is driven by multiple intestinal stem cell (ISC) types, including an active, radiosensitive Wnt^{high} ISC that fuels turnover during homeostasis and a reserve, radioresistant Wnt$^{low/off}$ ISC capable of generating active Wnt^{high} ISCs. We examined the role of the Msi family of oncoproteins in the ISC compartment. We demonstrated that Msi proteins are dispensable for normal homeostasis and self-renewal of the active ISC, despite their being highly expressed in these cells. In contrast, Msi proteins are required specifically for activation of reserve ISCs, where Msi activity is both necessary and sufficient to drive exit from quiescence and entry into the cell cycle. Ablation of Msi activity in reserve ISCs rendered the epithelium unable to regenerate in response to injury that ablates the active stem cell compartment. These findings delineate a molecular mechanism governing reserve ISC quiescence and demonstrate a necessity for the activity of this rare stem cell population in intestinal regeneration.

Introduction

Radiation-induced acute gastrointestinal syndrome is caused when the body is exposed to high doses of penetrating radiation (usually 10 Gy or higher). Mortality rates are high in these instances, as destructive damage in the gastrointestinal tract results in electrolyte imbalance and rapid dehydration. The molecular determinants of intestinal radiosensitivity and gastrointestinal syndrome are poorly understood. Intestinal stem cells (ISCs), which are crucial for physiological tissue homeostasis and regeneration after injury, are thought to play a critical role in this process (Potten, 2004; Ch'ang et al., 2005).

Crypt base columnar cells (CBCs) are highly proliferative stem cells that reside at the base of intestinal crypts. CBCs are characterized by high activity of the canonical Wnt pathway, and activity of the Wnt target gene *Lgr5* is commonly used for their identification and prospective isolation (Cheng and Leblond, 1974; Barker et al., 2007). Although CBCs are widely believed to maintain the daily proliferative burden of the high-turnover epithelium, they are sensitive to DNA damage–causing agents such as high-dose γ-irradiation (γ-IR), and several independent studies have demonstrated that CBCs are largely ablated after γ-IR (Hua et al., 2012; Yan et al., 2012; Metcalfe et al., 2014; Asfaha et al., 2015). Recently, Tao et al. (2015) showed that high Wnt pathway activity and basal crypt positioning sensitize CBCs to DNA damage, leading to their preferential depletion. Interestingly, that study also characterized a population of Wnt^{low}/Lgr5^{low} cells above the crypt base that appear more radioresistant, raising the possibility that the Lgr5-marked population is heterogeneous and that Lgr5^{low} cells may contribute to regeneration after irradiation. Another recent study showed that ablation of Lgr5-expressing cells by a diphtheria toxin receptor inserted into the endogenous *Lgr5* locus activated shortly before (or after) administration of high-dose radiation impairs the regeneration efficiency of the epithelium, suggesting a contribution from Lgr5^{+} cells to regeneration after radiation injury, although the timing of diphtheria toxin administration makes it difficult to dissect the contribution of radioresistant versus de novo–generated Lgr5^{+} cells to the regenerative process (Metcalfe et al., 2014).

Despite the loss of the vast majority of Wnt^{high} CBCs after high-dose γ-IR, regenerative crypt foci begin appearing ∼2–3 d after γ-IR exposure and fully repair the epithelium within ∼5 d. This regeneration is believed to be driven by a population of radioresistant stem cells with little to no canonical Wnt pathway activity (referred to hereafter as "reserve ISCs"). At least some of these reserve ISCs can be marked by *CreER* reporter genes targeted to the endogenous *Bmi1* and *Hopx* loci

Correspondence to Christopher J. Lengner: lengner@vet.upenn.edu

Abbreviations used: CBC, crypt base columnar cell; DKO, double knockout; EdU, ethynyl deoxyuridine; FDR, false discovery rate; γ-IR, γ-irradiation; ISC, intestinal stem cell; LT-HSC, long-term hematopoietic stem cell.

The Rockefeller University Press $30.00
J. Cell Biol. Vol. 215 No. 3 401–413
https://doi.org/10.1083/jcb.201604119

(Sangiorgi and Capecchi, 2008; Takeda et al., 2011; Yan et al., 2012; Li et al., 2014); however, recent evidence suggests that more differentiated cells may also act as facultative stem cells upon ablation of CBCs (Tetteh et al., 2016). Despite the lack of consensus on the precise populations contributing to regeneration after injury, clear evidence demonstrates that under basal conditions in the absence of injury, *Bmi1-/Hopx-CreER*–marked reserve ISCs give rise to CBCs. Lineage tracing coupled with single-cell gene expression profiling reveals that *Bmi1-/Hopx-CreER* alleles mark a largely overlapping population of Wnt^{-} reserve ISCs that give rise to active, Wnt^{high} $Lgr5^{+}$ CBCs upon division, and consequently all functional cell types of the epithelium over long periods of time (Takeda et al., 2011; Tian et al., 2011; Yan et al., 2012; Li et al., 2014). Unlike $Lgr5^{+}$ CBCs, the population of reserve ISCs is largely quiescent (in G0 and metabolically inactive) rather than activated (metabolically active and within the cell cycle; Li et al., 2016). It has been postulated that the low metabolic activity of quiescent stem cells discourages genetic lesions induced by reactive oxygen species (Pazhanisamy, 2009). However, knowledge of the molecular mechanisms governing their radioresistance and subsequent exit from the quiescent state in response to γ-IR injury is lacking.

Musashi (Msi) RNA-binding proteins are expressed in the stem cell compartments of several tissues including the brain, intestine, and blood and are up-regulated in cancers arising from these tissues (Park et al., 2014; Li et al., 2015; Wang et al., 2015). Msi proteins act primarily as translational regulators binding to messenger RNAs, and known target transcripts are involved in the regulation of cell cycle progression, metabolism, and stem cell self-renewal (Park et al., 2014; Li et al., 2015; Wang et al., 2015). In the hematopoietic system, Msi2 is an important modulator of long-term hematopoietic stem cell (LT-HSC) proliferation and self-renewal (Hope et al., 2010; Ito et al., 2010; Kharas et al., 2010; Park et al., 2014). Ectopic induction of Msi2 increases LT-HSC numbers, which is associated with a reduction in stem cell quiescence and a concomitant increase in the percentage of actively cycling LT-HSCs (Kharas et al., 2010). Conversely, *Msi2* deletion results in loss of engraftment potential of LT-HSCs in transplantation assays, demonstrating the importance of Msi2 in this largely dormant stem cell population (Park et al., 2014).

In the intestinal epithelium, Msi proteins are expressed throughout the crypt, including in the active CBC stem cell compartment (Itzkovitz et al., 2011; Li et al., 2014, 2015; Wang et al., 2015). We have previously established that Msi proteins are obligate and functionally redundant intestinal oncoproteins that drive epithelial transformation in large part through inhibition of intestinal tumor suppressors including Pten, resulting in downstream mTORC1 complex activation (Li et al., 2015; Wang et al., 2015); however, their role in intestinal homeostasis, regeneration, and stem cell self-renewal in vivo is entirely unknown. Here, we establish that Msi proteins are dispensable for the Wnt-driven self-renewal of CBCs but are required for cell cycle entry of quiescent reserve ISCs residing in G0. Msi up-regulation in reserve ISCs is sufficient to induce expression of metabolic genes including *Myc*, *H6pd*, and *Hif1α* and drive exit of reserve ISCs from G0 and into the cell cycle. Conversely, genetic ablation of *Msi* genes abrogates cell cycle entry. This manifests phenotypically in the failure of epithelial regeneration in response to injury. Further, we demonstrate that Msi expression must be tightly regulated in quiescent ISCs, as premature Msi induction before γ-IR injury sensitizes the intestinal epithelium to injury and impairs regenerative capacity. This emphasizes the importance of maintaining a pool of quiescent stem cells for the tissue to mount an effective injury response.

Results

Msi activity is dispensable for intestinal homeostasis, Wnt pathway activity, and CBC function under basal conditions

We initially confirmed published studies of Msi expression in the intestinal crypt, where Msi1 and Msi2 are expressed in CBCs and the transit-amplifying zone (Fig. 1 A; Li et al., 2015). To unequivocally test the functional contribution of Msi proteins to intestinal homeostasis and stem cell self-renewal, we intercrossed *Msi1* and *Msi2* conditional knockout alleles previously generated in our laboratory (Katz et al., 2014; Park et al., 2014; Li et al., 2015; Wang et al., 2015) with mice harboring a *Villin-CreER* transgene that drives robust, inducible recombination throughout all epithelial cells in the small intestine and colon (el Marjou et al., 2004; Li et al., 2015). Ablation of either *Msi1* or *Msi2* individually throughout the intestinal epithelium and colon had no effect on tissue homeostasis, proliferation, or differentiation (not depicted), consistent with published studies demonstrating their functional redundancy (Sakakibara et al., 2002; Li et al., 2015).

We therefore examined the consequences of concomitant ablation of both *Msi1* and *Msi2* in $Msi1^{flx/flx}$::$Msi2^{flx/flx}$::*Villin-CreER* double knockout (*Msi-DKO*) mice. We followed *Msi-DKO* mice for 1 wk and up to 6 mo after deletion and, surprisingly, observed no overt phenotypic changes to intestinal crypt–villus architecture (Fig. 1 B), alteration in proliferation (Figs. 1 C and S1 A), or differentiation based on the frequency of Paneth and goblet cells (Fig. S1, B and C). We also examined the colon in *Msi-DKO* and control mice and similarly observed no phenotypic changes (Fig. S2, A and B) or alteration in proliferation (Fig. S2 C).

Transcriptome profiles from the crypts of control and *Msi-DKO* mice 1 wk after *Msi* deletion with *Villin-CreER* showed little differential gene expression, consistent with the phenotypic analysis. The few genes with significant changes in expression (fold change ≥1.5, p-value ≤0.1) were not enriched for any specific functional ontology (Table S1). Importantly, loss of Msi activity had no deleterious consequences for expression of Wnt pathway target genes, which is critical for proper intestinal homeostasis and CBC proliferation (Fig. 1 D). In addition, ablation of *Msi1*, *Msi2,* or both had no effect on nuclear localization of the Wnt transcriptional effector β-catenin in cells at the crypt base (Fig. S2 D). Further, we were able to generate *Msi*-null crypt organoids in vitro and passage them serially with no decrease in organoid-forming efficiency or detectable increase in *Msi* expression, which would be expected to result from selective pressure if rare cells escaping recombination had a growth advantage (Figs. 1 E and S2 E). There was also no difference in organoid-forming efficiency between *Msi-DKO* and control crypts at any R-spondin concentration tested in the absence of GSK-3 inhibitor (Fig. 1 E). These findings demonstrate that Msi does not support activity of the canonical Wnt pathway and are in contrast to in vitro studies and in vivo gain-of-function assays suggesting that Msi potentiates activity of this pathway (Rezza et al., 2010; Spears and Neufeld, 2011; Cambuli et al., 2015).

Ultimately, we tested the effects of Msi loss on the activity of CBCs marked by an *Lgr5-eGFP-CreER* reporter allele

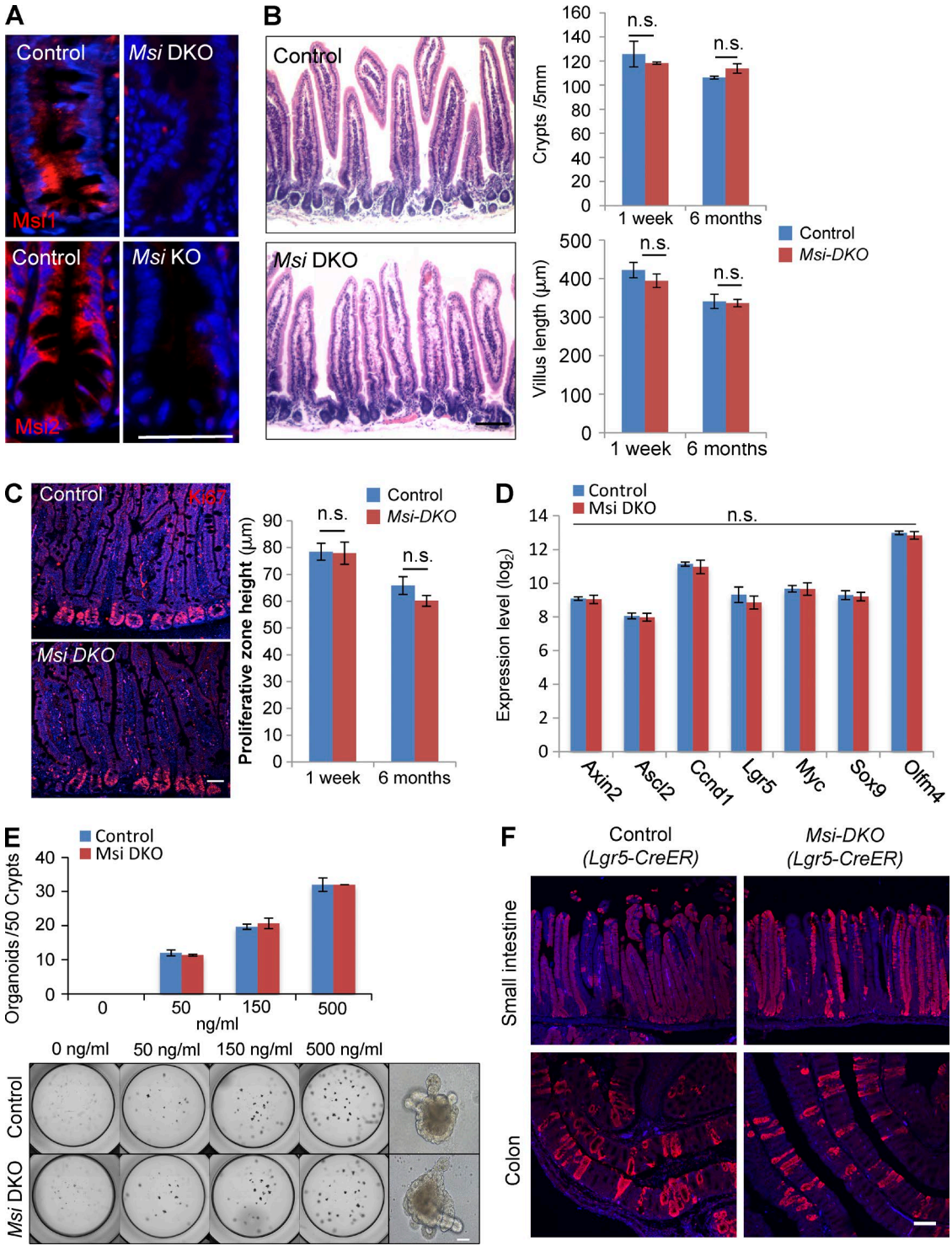

Figure 1. **Msi activity is dispensable for intestinal homeostasis, Wnt pathway activity, and CBC function under basal conditions.** *Msi1/2*$^{flx/flx}$*::Villin-CreERT2* (*MSI DKO*) and control mice were given five consecutive daily doses of tamoxifen and harvested either 1 wk or 6 mo later (n = 3–5). (A) Msi1 and Msi2 staining in normal intestinal crypts under basal conditions in control and *Msi-DKO* mice. Bar, 50 µM. (B) Hematoxylin and eosin–stained sections from the jejunum of mice 6 mo after tamoxifen injection; quantification of number of crypts per unit length of small intestine and length of villi based on these hematoxylin and eosin–stained sections. Bar, 100 µM. (C) Ki67 staining of sections from jejunum of mice; measurement of length of proliferative zone based on these Ki67-stained sections. Bar, 50 µM. (D) Gene expression analysis of Wnt pathway target genes of crypts isolated from *Msi1/2*$^{flx/flx}$*::Villin-CreER* and control mice 1 wk after tamoxifen treatment (n = 3). (E) Organoid formation assay with crypts isolated from *Msi1/2*$^{flx/flx}$*::Villin-CreER* and control mice cultured with increasing doses of R-spondin in the absence of GSK-3 inhibitor. 50 crypts were initially plated per well (n = 3). Bar, 50 µM. (F) Immunofluorescence staining for tdTomato in sections of small intestine and colon of *Lgr5-eGFP-IRES-CreER::LSL-tdTomato::Msi1/2*$^{flx/flx}$ mice and their control counterparts 14 d after activating the tdTomato reporter and deleting *Msi* genes with tamoxifen. Bar, 50 µm. All data are expressed as mean ± SD. *, P < 0.05; **, P < 0.005; ***, P < 0.0005, Student's *t* test; n.s., not significant.

(Barker et al., 2007). Msi loss had no effect on the frequency or proliferation of CBCs (Fig. S2, F and G). In addition, lineage tracing in *Lgr5-eGFP-CreER::Msi1$^{flx/flx}$::Msi2$^{flx/flx}$::R26-Lox-Stop-Lox-tdTomato* or control (*Lgr5-eGFP-CreER::R26-Lox-Stop-Lox-tdTomato)* mice demonstrated that Msi loss has no detrimental consequences for CBC stem cell activity in vivo, in either the small intestine or colon (Figs. 1 F and S2 H). We confirmed efficient deletion of *Msi1/2* in Lgr5^{+} ISCs and their progeny (Fig. S2, I and J). Collectively, these findings demonstrate that Msi loss has no effect on the activity of the canonical Wnt pathway or the proliferative self-renewal of CBCs.

Msi proteins are required for intestinal regeneration after radiation injury

Given prior findings demonstrating that Msi1/2 activity potentiates the activity of the mTORC1 complex in colorectal cancer (Li et al., 2015; Wang et al., 2015), and that mTORC1 is similarly dispensable for intestinal homeostasis but is required for epithelial regeneration in response to injury (Ashton et al., 2010; Faller et al., 2015), we next sought to determine how Msi loss affects intestinal regeneration in response to radiation injury. *Msi1$^{flx/flx}$::Msi2$^{flx/flx}$::Villin-CreER* or control *Msi1$^{flx/flx}$::Msi2$^{flx/flx}$* mice were treated with five daily doses of tamoxifen and subjected to 12 Gy of ionizing γ-IR 1 wk later to ablate proliferative cells including CBCs (Tian et al., 2011; Tao et al., 2015). In this context, intestinal regeneration (quantified by the number of clonal regenerative crypt foci per unit length 72 h after injury) was severely compromised in the absence of Msi activity (Fig. 2 A and Fig. S3 A). No differences in the distribution of residual differentiated cell types were observed (Fig. S3, B and C). Any regenerative crypt foci observed in *Msi1$^{flx/flx}$::Msi2$^{flx/flx}$::Villin-CreER* mice were found to have escaped recombination at one or more of the floxed *Msi* alleles (Fig. 2 B). These data demonstrate that Msi activity is necessary for regeneration of the epithelium.

Recent studies indicate that the regenerative capacity of the epithelium in response to such high-dose γ-IR resides in a population of reserve intestinal ISCs that are marked, at least in part, by *Hopx-CreER* or *Bmi1-CreER* alleles (and possibly by other proxy reporter alleles; Montgomery et al., 2011; Takeda et al., 2011; Yan et al., 2012; Metcalfe et al., 2014; Asfaha et al., 2015). *Bmi1-* or *Hopx-CreER* reporters are known to mark a largely overlapping population of rare reserve ISCs (although the *Hopx-CreER* population is more homogeneous; Li et al., 2014). We next asked, therefore, whether *Msi* ablation specifically in this rare reserve ISC population could account for the failed regenerative response we observed after *Msi* ablation throughout the epithelium using *Villin-CreER*. To address this question, we crossed the *Hopx-CreER* allele into *Msi1$^{flx/flx}$::Msi2$^{flx/flx}$* mice and assessed regeneration of intestinal epithelium after deletion of Msi using *Villin-CreER*, *Hopx-CreER*, or *Lgr5-CreER* and exposure to 12 Gy γ-IR. Msi ablation with *Lgr5-CreER* had no significant effect on regeneration, although a modest, nonsignificant decrease in regeneration was observed, possibly reflecting the function of an *Lgr5*^{low} cell previously described as radioresistant (Tao et al., 2015). In contrast, *Msi* loss in rare *Hopx-CreER* reserve ISCs (making up less than 0.5% of the crypt epithelium; Takeda et al., 2011; Li et al., 2014) and some of their immediate progeny (as some reserve ISCs must divide during the time required for multiple tamoxifen injections before irradiation) resulted in failed epithelial regeneration to an extent indistinguishable from that observed with panepithelial *Villin-CreER* deletion, highlighting the importance of these rare reserve ISCs in the regenerative response of the intestinal epithelium (Fig. 2 C).

Msi activity selectively governs reserve stem cell proliferation

Although these findings demonstrate that *Hopx-/Bmi1-CreER* reserve ISCs are important for epithelial regeneration after injury, recent data also suggest that the more differentiated progeny of *Lgr5*$^{+}$ CBCs can revert to the CBC state and reacquire stem cell activity after CBC ablation with diphtheria toxin (Tetteh et al., 2016). Under basal, noninjury conditions, *Hopx-/Bmi1-CreER* ISCs are known to give rise to *Lgr5*$^{+}$ CBCs upon division (Takeda et al., 2011; Tian et al., 2011; Li et al., 2014). We thus sought to examine whether Msi plays an important role in the activation of these reserve ISCs during basal homeostasis. We initially performed single-cell gene expression analysis in *Lgr5*$^{+}$ CBCs, reserve ISCs, and the progeny of reserve ISCs after 4 d of lineage tracing. As predicted, in the resting state, reserve ISCs marked by *Hopx-/Bmi-CreER::R26-Lox-Stop-Lox-tdTomato* reporter activity 18 h after a single tamoxifen dose (Takeda et al., 2011; Li et al., 2014) expressed low levels of *Msi* genes and existed in a Wnt$^{off/low}$ state, with little to no expression of canonical Wnt targets such as *Lgr5*, *Ascl2*, and *Ccnd1*, along with high levels of the cell cycle inhibitor *Cdkn1a*, in stark contrast to CBCs (Fig. 3, A and B). Four days after initiation of lineage tracing (when about half of reserve ISCs have divided to form clusters of two or more daughter cells; Takeda et al., 2011; Li et al., 2014), reserve ISC progeny began activating Msi genes and canonical Wnt target genes (Fig. 3 B). These data further suggest that Msi activity plays a role in promoting reserve ISC cell cycle entry.

To test this definitively, we examined lineage tracing from control mice (*Hopx-/Bmi1-CreER::R26-Lox-Stop-Lox-tdTomato*) or mice in which Msi activity is ablated specifically in reserve ISCs (*Msi1$^{flx/flx}$::Msi2$^{flx/flx}$*::*Hopx-/Bmi1-CreER::R26-Lox-Stop-Lox-tdTomato*). As predicted based on previous studies and single-cell gene expression analysis (Fig. 3 B), reserve ISCs in control mice gave rise to clonal lineage tracing events that encompassed the entire crypt–villus axis after 14 d. In contrast, Msi loss abrogated lineage tracing from reserve ISCs, and these cells remained as single-labeled cells within intestinal crypts 14 d after initiation of tracing (Fig. 3 C, arrowheads). These findings demonstrate that Msi activity is required for reserve ISC activation under basal homeostatic conditions, in which these cells normally generate CBCs.

Reserve ISCs represent a quiescent stem cell pool residing in G0 and require Msi activity for S-phase entry

Recent findings that high Wnt pathway activity and cell cycling render CBCs susceptible to DNA damage (Tao et al., 2015) support a model in which a more dormant pool of reserve stem cells remains resistant to injury to regenerate the epithelium after damage. These reserve stem cells are often referred to as quiescent (i.e., residing in the G0 state outside of the cell cycle). We therefore sought to characterize quiescence in reserve ISCs. In stem cell biology, quiescence usually refers to cells with a dormant genome and low metabolic activity, reflected by low RNA levels in a diploid cell (G0), rather than simply the absence of cycling, which can also result from G1 arrest (Hüttmann et al., 2001; Fukada et al.,

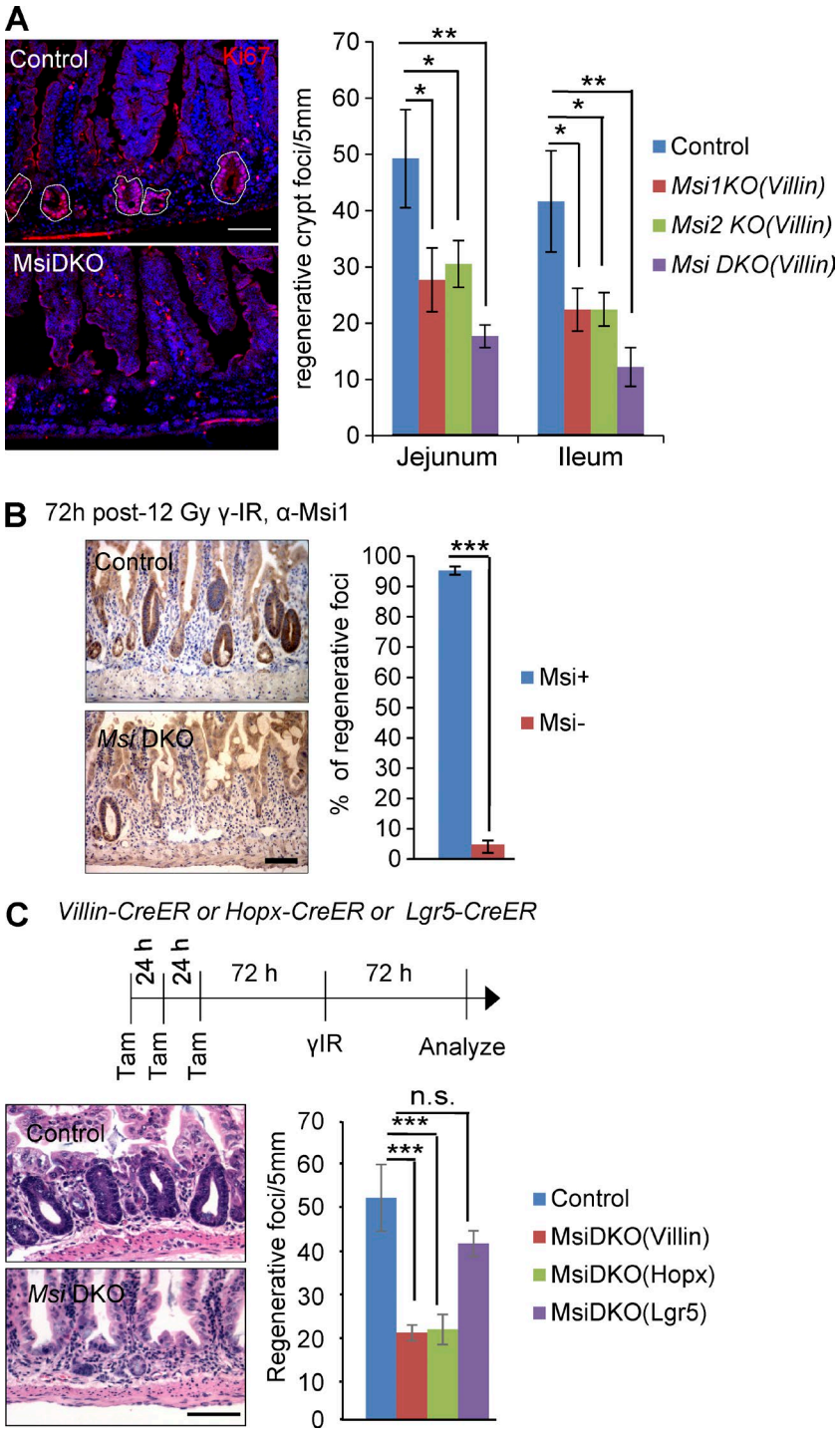

Figure 2. **Msi loss abrogates epithelial regeneration after γ-IR injury.** (A) Representative Ki67-stained sections from jejunum of irradiated *Msi1/2*$^{flx/flx}$*::Villin-CreER* and control mice; quantification of number of proliferative crypt foci per unit length of small intestine. All groups of mice were given five daily consecutive doses of tamoxifen and were exposed to 12 Gy γ-IR 1 wk later. Tissue was harvested 3 d after γ-IR (n = 5–6). Bar, 100 µM. (B) Msi1-stained sections from jejunum of mice described in A; quantification of percentage of regenerative crypts escaping recombination based on Ki67- and Msi (Msi1/2)-stained serial sections. (C) *Msi1/2*$^{flx/flx}$*::Villin-CreER*, *Msi1/2*$^{flx/flx}$*::Hopx-CreER*, and *Msi1/2*$^{flx/flx}$*::Lgr5-CreER* and control mice were given three consecutive doses of tamoxifen (Tam), 24 h apart, and were exposed to 12 Gy γ-IR 3 d after the final dose. Tissue was harvested 3 d after γ-IR. Hematoxylin and eosin–stained sections from the jejunum were used for quantification of regeneration efficiency (regenerative crypt foci per unit length of small intestine; n = 4–6). Bar, 100 µM. All data are expressed as mean ± SD. *, P < 0.05; **, P < 0.005; ***, P < 0.0005, Student's t test; n.s., not significant.

2007). We first examined reserve ISC populations marked by *Hopx-/Bmi1-CreER::R26-Lox-Stop-Lox-tdTomato* and found that the majority of these populations reside in G0 (Fig. 4 A). Exposure of these mice to 12 Gy γ-IR resulted in an exit of reserve ISCs from G0 into the cell cycle concomitant with an increase in Msi (Fig. 4, B and C; and Fig. S4, A and B), consistent with the previous functional demonstration that Msi activity in these cells is important for effective regeneration. We next asked how Msi loss affected the quiescent status of the reserve ISC compartment. Interestingly, ablation of Msi in reserve ISCs resulted in a G1 (not G0) arrest (Fig. 4 D). Further, these cells were no longer able to enter S-phase and incorporate ethynyl deoxyuridine (EdU) in response to 12 Gy γ-IR (Fig. 4, D and E). Interestingly, these findings are consistent with previous studies on the mTORC1 complex, inactivation of which similarly results in G1 arrest (Kalaitzidis et al., 2012) as well as failure of the intestinal epithelium to regenerate in response to high dose γ-IR injury (Ashton et al., 2010; Faller et al., 2015).

Collectively, the findings thus far demonstrated that reserve ISCs represent a pool of quiescent stem cells that require induction of Msi activity for proper exit from quiescence and

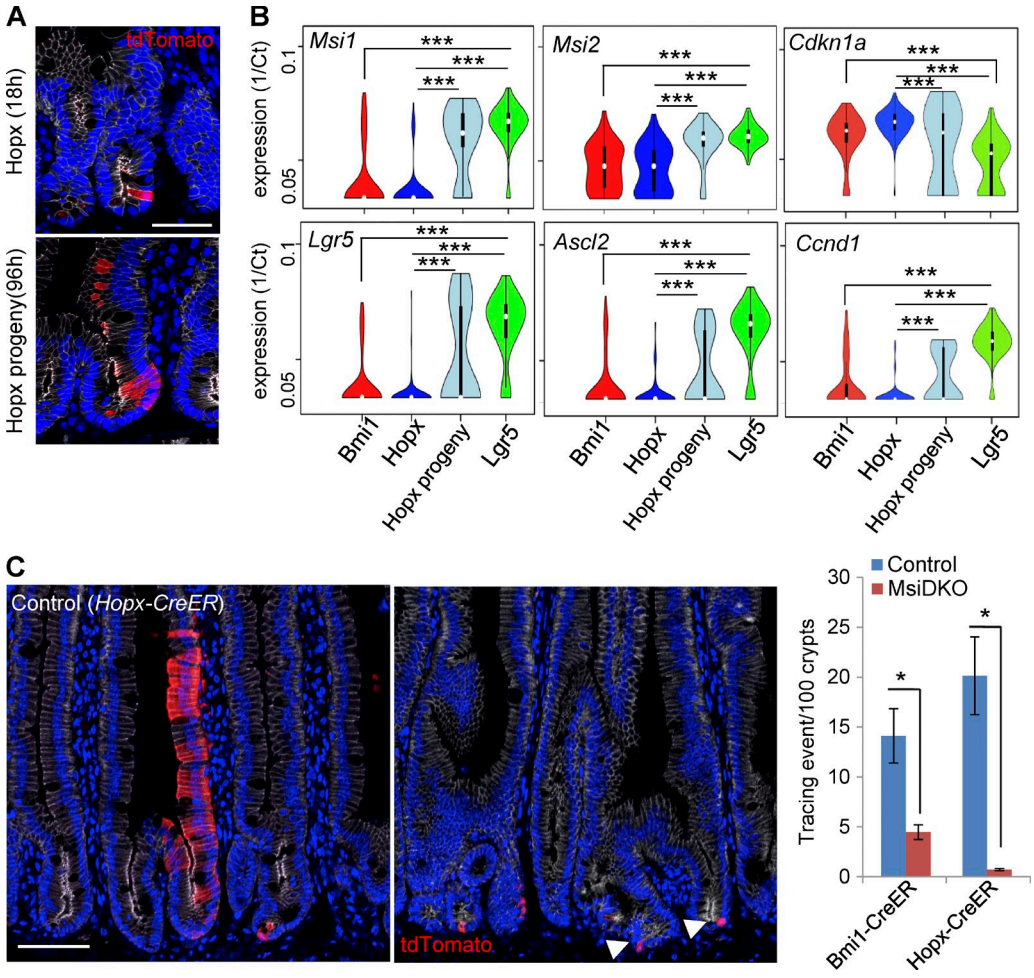

Figure 3. **Msi is up-regulated during activation of reserve ISCs and is required for lineage tracing from these cells under basal conditions.** (A) Representative immunofluorescence micrographs of *Hopx-CreER* reserve ISCs and their progeny in *Hopx-CreER::LSL-tdTomato* mice 18 h (top) and 4 d (bottom) after a single tamoxifen injection. TdTomato (red), E-cadherin (white), and DAPI (blue). Bar, 50 µM. (B) Violin plots showing expression levels of *Msi1*, *Msi2*, *Lgr5*, *Ascl2*, *Cdkn1a*, and *Ccnd1* in single, FACS-purified *Bmi1*- and *Hopx-CreER* ISCs, their daughter cells (progeny), and *Lgr5-eGFP*$^{+}$ CBCs. *Bmi1*- and *Hopx-CreER*$^{+}$ ISCs were marked by a single dose of tamoxifen in *Bmi1- or Hopx-CreER::LSL-tdTomato* mice and were purified by FACS 18 h later. *Hopx-CreER* progeny were isolated by FACS purification of tdTomato^{+} cells 96 h after activation of the *tdTomato* reporter. The width of the violin plot represents the number of single cells at the given expression level on the *y*-axis. The white dot within the violin plot represents the mean expression value for the group of cells. (C) Immunofluorescence staining for tdTomato (red) and E-cadherin (white) and quantification of lineage tracing events (ribbons of tdTomato^{+} cells with contiguous tracing from crypts, through crypt–villus junction, and into villi) from *Bmi1*- and *Hopx-CreER* ISCs 14 d after marking reserve ISCs with a single tamoxifen injection to *Hopx-CreER::LSL-tdTomato::Msi1/2*$^{flx/flx}$ or *Bmi1-CreER::LSL-tdTomato::Msi1/2*$^{flx/flx}$ mice and their control counterparts (n = 3). Bar, 50 µM. Arrowheads point to single *MsiDKO* cells that are not able to contribute in lineage tracing. All data are expressed as mean ± SD. *, P < 0.05; ***, P < 0.0005, Student's *t* test.

cell cycle entry, which in turn is necessary for regeneration of the epithelium in response to injury.

Msi activity is sufficient to drive reserve ISCs out of G0 and into the cell cycle

We next asked whether Msi activity alone was sufficient to drive reserve ISC exit from G0 and into the cell cycle. To address this question, we used a mouse model in which a single copy of Msi1 is targeted into safe-haven chromatin and is under control of the doxycycline-inducible tetracycline-responsive element (*TRE-Msi1*; Li et al., 2015). Administration of doxycycline to *Hopx-/Bmi1-CreER::R26-Lox-Stop-Lox-tdTomato::TRE-Msi1* mice for as little as 36 h resulted in robust exit of reserve ISCs from G0 and subsequent entry into the cell cycle (Fig. 5 A). This ectopic Msi induction drove increased proliferation and lineage tracing from reserve ISCs (Fig. 5, B–D). At the molecular level, Msi induction activated expression of metabolic and proliferative genes such as *H6pd*, *Hif1α*, and *c-Myc* in reserve ISCs (Fig. 5 E, Fig. S5 A, and Table S2). In contrast, ectopic Msi induction did not induce expression of canonical Wnt target genes such as *Lgr5* and *Ascl2* in reserve ISCs (Fig. 5 E). Further, ectopic Msi induction had no effect on the molecular identity of CBCs, further confirming the cell type specificity of Msi function (Fig. 5, E and F). These findings indicate that Msi drives reserve stem cells out of quiescence in a Wnt-independent manner.

Premature exit of reserve ISCs from G0 sensitizes the intestinal epithelium to radiation injury

Ultimately, the data presented thus far led to a model in which reserve ISCs maintain radioresistance by virtue of their residence in the quiescent G0 state outside of the cell cycle in the absence of Msi activity. Under basal conditions, Msi is periodically

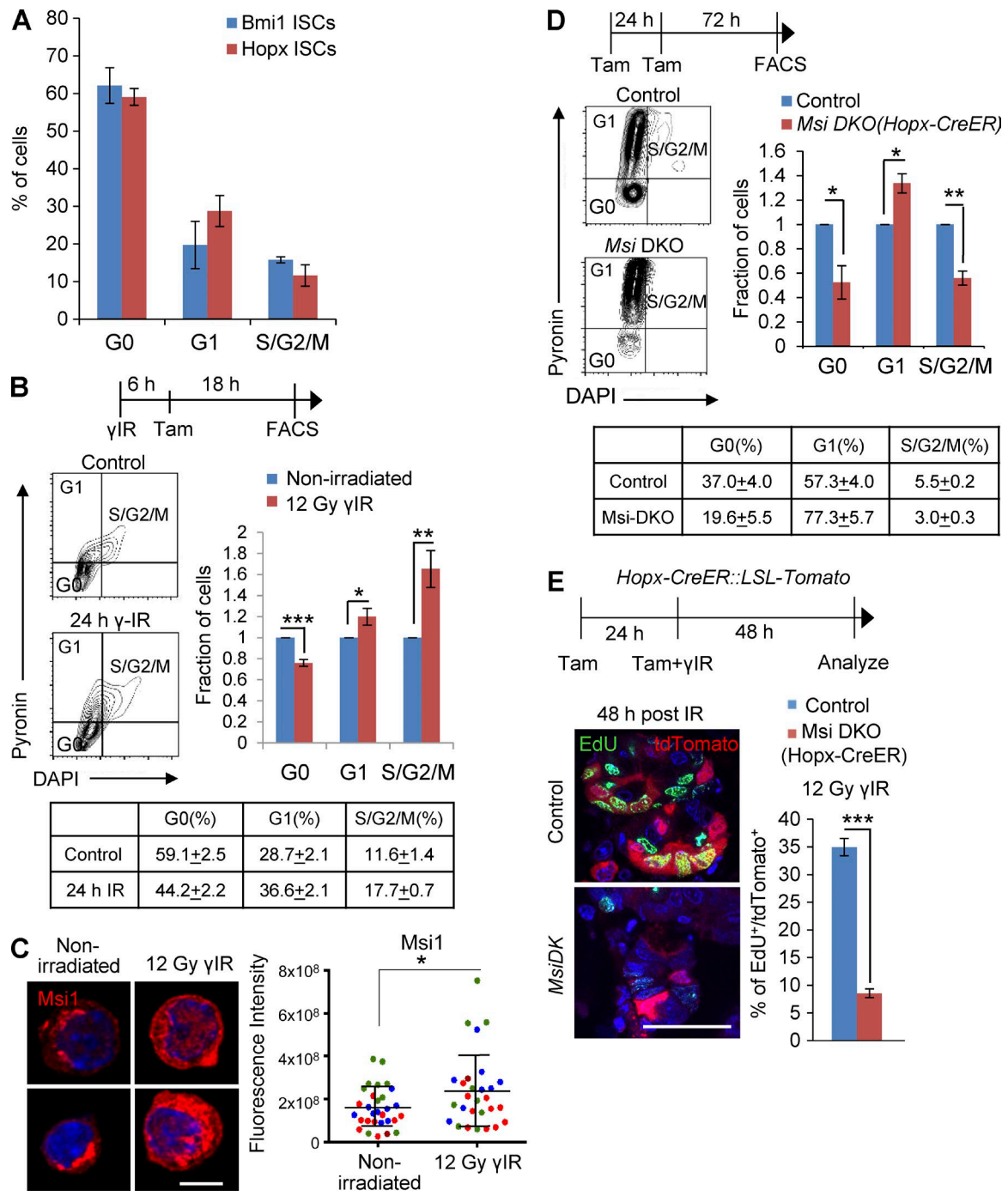

	G0(%)	G1(%)	S/G2/M(%)
Control	59.1±2.5	28.7±2.1	11.6±1.4
24 h IR	44.2±2.2	36.6±2.1	17.7±0.7

	G0(%)	G1(%)	S/G2/M(%)
Control	37.0±4.0	57.3±4.0	5.5±0.2
Msi-DKO	19.6±5.5	77.3±5.7	3.0±0.3

Figure 4. **Msi is up-regulated after radiation injury coupled with exit of reserve ISCs from quiescence into cell cycle.** (A) Analysis of cell cycle distribution of different reserve ISC populations using pyronin Y and DAPI staining in *Bmi1-CreER::LSL-tdTomato* and *Hopx-CreER::LSL-tdTomato* mice, 18 h after tamoxifen (Tam) injection. Cell cycle distribution was determined using pyronin Y and DAPI staining during homeostasis. Pyronin Y^{low} $DAPI^{low}$ (2n) cells: G0; pyronin Y^{high} $DAPI^{low}$ (2n) cells: G1; and pyronin Y^{high} $DAPI^{high}$ cells (>2n DNA content): G2/M (n = 3). (B) Analysis of quiescence in *Hopx-CreER*$^+$ ISCs using pyronin Y and DAPI staining under basal conditions and 24 h after 12 Gy γ-IR. To mark *Hopx-CreER* ISCs, mice were injected with tamoxifen 18 h before harvest (n = 4–5). (C) Immunofluorescence staining for Msi1 and quantification of Msi1 fluorescence intensity in *Hopx-CreER*$^+$ ISCs, 48 h after irradiation and 18 h after tamoxifen induction. Shown are micrographs of individual FACS-purified ISCs. Colored dots in the graph at right represent individual *Hopx-CreER*$^+$ ISCs isolated from three different pairs of irradiated and nonirradiated control mice (n = 3). Bar, 5 µM. (D) Analysis of cell cycle distribution of FACS-purified tdTomato$^+$ cells from *Hopx-CreER::LSL-tdTomato::Msi1/2*$^{flx/flx}$ or control mice 3 d after the second of two daily consecutive tamoxifen doses given during homeostasis (n = 3–4). (E) EdU-stained sections from the jejunum of *Msi1/2*$^{flx/flx}$*::LSL-tdTomato::Hopx-CreER* and control mice treated with two daily doses of tamoxifen. The mice were divided in two groups, and one group received 12 Gy γ-IR immediately after the second dose of tamoxifen. Tissue was harvested 2 d after the second dose of tamoxifen. The graph shows EdU incorporation of tdTomato$^+$ 48 h after IR in either the presence or absence of Msi (n = 3). Bar, 50 µM. All data are expressed as mean ± SD. *, P < 0.05; **, P < 0.005; ***, P < 0.0005, Student's t test.

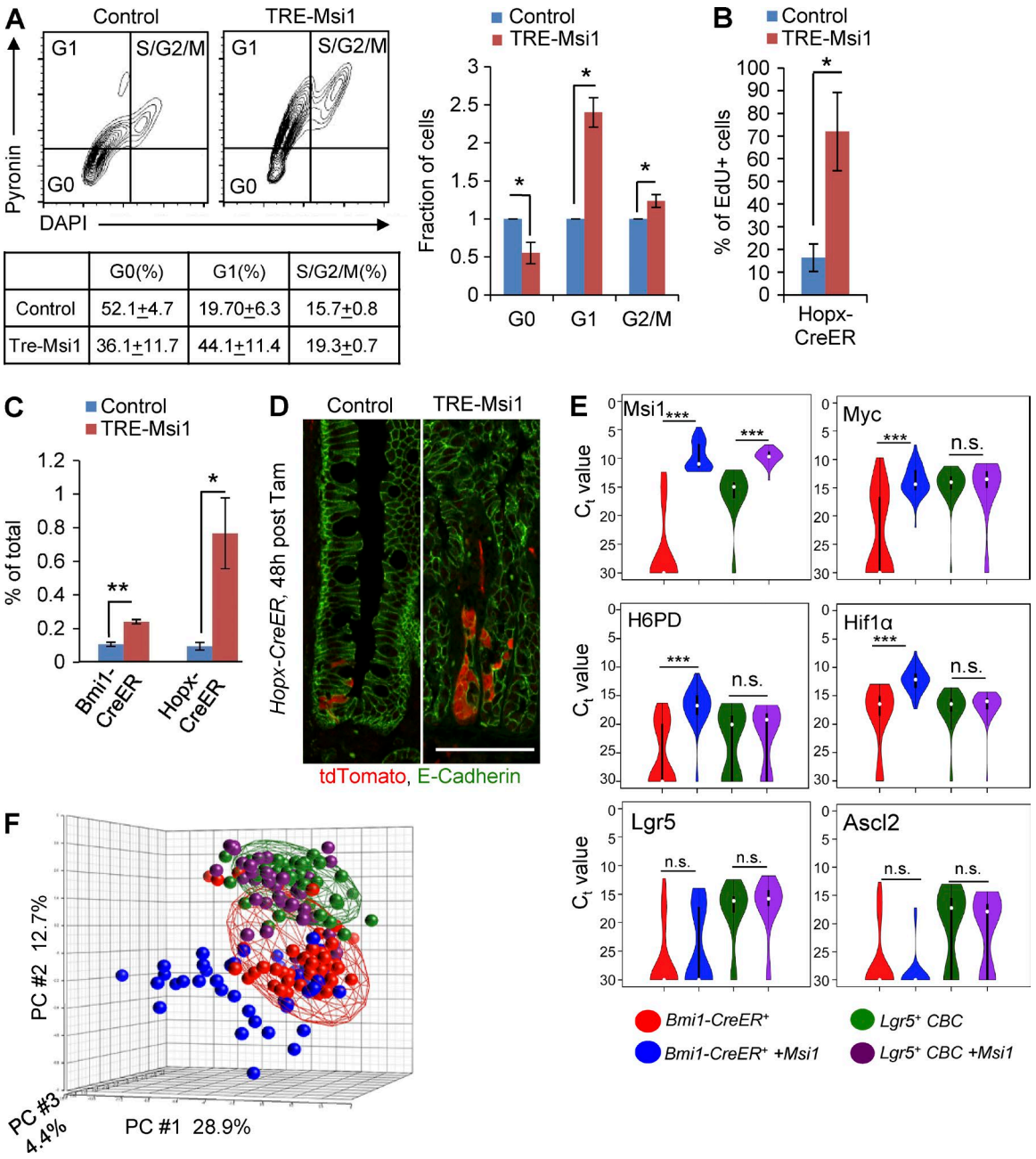

	G0(%)	G1(%)	S/G2/M(%)
Control	52.1±4.7	19.70±6.3	15.7±0.8
Tre-Msi1	36.1±11.7	44.1±11.4	19.3±0.7

Figure 5. **Msi up-regulation is sufficient to activate metabolic genes in reserve ISCs and drive these cells out of quiescence into the cell cycle.** (A) Analysis of cell cycle distribution of *Bmi1-CreER* ISCs 36 h after induction of Msi1 expression in *TRE-Msi1::Bmi1-CreER::tdTomato* and *Bmi1-CreER::tdTomato* control mice. Both *TRE-Msi1* and control (*R26-m2rtTA*) groups were treated with doxycycline in their drinking water for 18 h then given one dose of tamoxifen and maintained on doxycycline for an additional 18 h before tissue harvest ($n = 4$). (B) Assessment of EdU incorporation in *Hopx-CreER* ISCs from doxycycline- and tamoxifen-treated *TRE-Msi1::Hopx-CreER::tdTomato* and control (*R26-m2rtTA* + doxycycline) mice as described in A ($n = 4–5$). (C) Quantification of frequency of *Hopx-* and *Bmi1-CreER*$^+$ ISCs from doxycycline-treated (total 36 h) and tamoxifen-treated (18 h before tissue harvest) *TRE-Msi1::Hopx-CreER::tdTomato*, *TRE-Msi1::Bmi1-CreER::tdTomato*, and control (*R26-m2rtTA* + doxycycline) mice ($n = 3–4$). (D) Lineage tracing from *Hopx-CreER* ISCs staining for tdTomato in sections from *Tre-Msi1::Hopx-CreER::tdTomato* and control (*R26-m2rtTA* + doxycycline) mice 48 h after doxycycline and tamoxifen treatment. Bar, 50 µM. (E) Violin plots showing expression levels in populations of single ISCs. The white dot in the violin plot represents the median expression within the group of cells, the black box represents the interquartile range, and the width of the plot is directly correlated to the number of cells at the given expression level indicated on the *y*-axis. (F) Principal component analysis of cellular identity in single *Lgr5-eGFP*^{High} CBCs and quiescent (*Bmi1-CreER*$^+$) ISCs with and without Msi1 induction based on the expression profiling of 48 transcripts representing the Wnt pathway, Notch pathway, proliferation, metabolism, and stem cell identity. Each sphere represents a single cell, and the percentage of variation ascribed to each of the principle components is delineated on the axes. The cages around the *Bmi1-CreER* (red) and *Lgr5-eGFP* (green) populations represent the domain contained within two SDs of the arithmetic centroid of the population. Color coding of ISCs is indicated in the panel. All data are expressed as mean ± SD. *, $P < 0.05$; **, $P < 0.005$; ***, $P < 0.0005$, Student's *t* test; n.s., not significant.

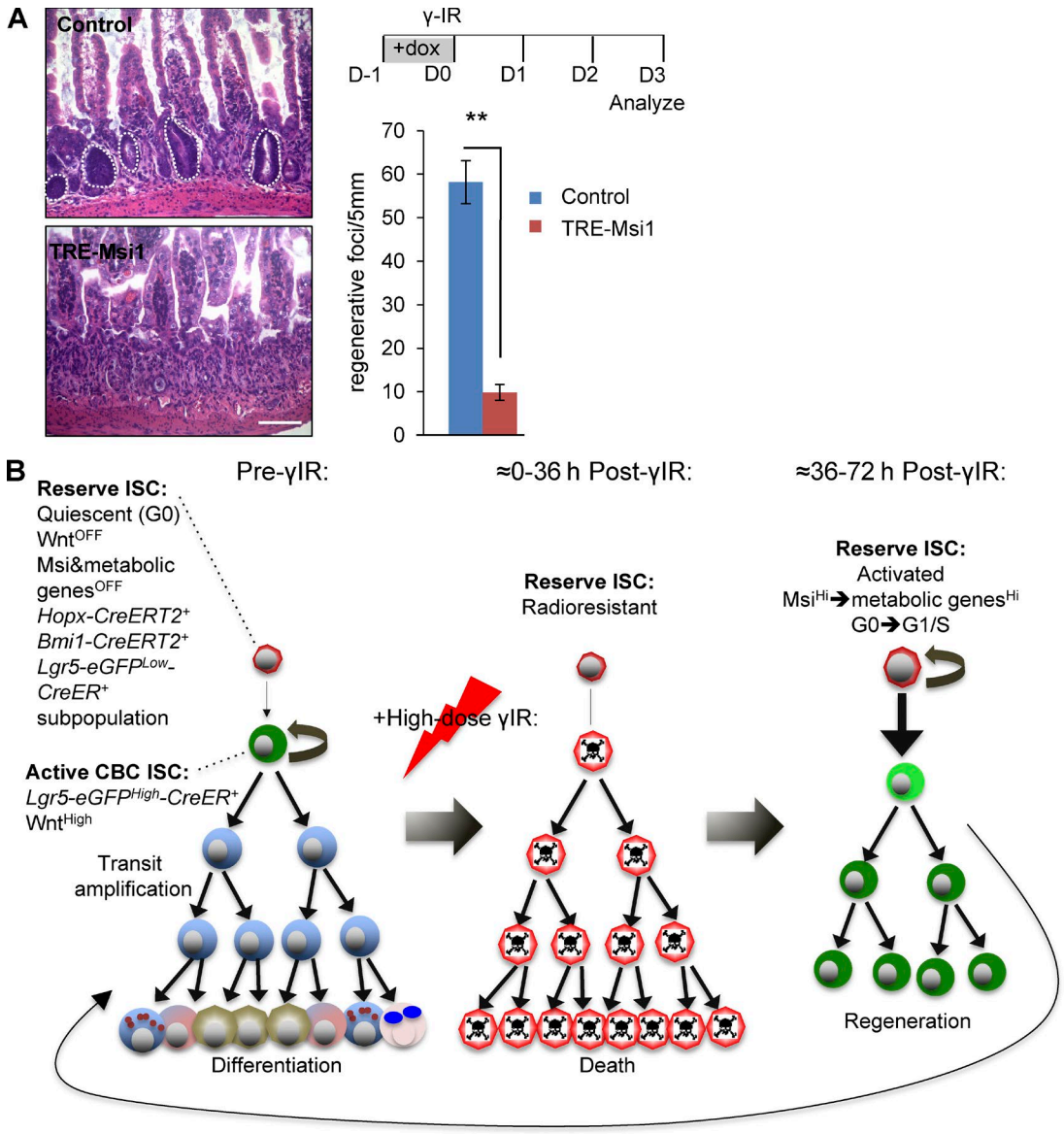

Figure 6. **Msi activity regulates radiosensitivity of intestinal epithelium.** (A) Hematoxylin and eosin–stained sections from the jejunum of irradiated *TRE-Msi1* and control (*R26-m2rtTA*) mice. Both groups received doxycycline for 24 h before irradiation and were harvested 3 d after γ-IR. During the regeneration period, mice received regular drinking water (no doxycycline). Quantification of regeneration efficiency after irradiation injury was done by counting regenerative crypt foci, defined as 10 or more adjacent chromophilic cells and a lumen in hematoxylin and eosin–stained sections (n = 3–4). Bar, 100 µm. (B) Model depicting behavior of reserve and active ISCs during homeostasis and regeneration after high-dose γ-IR. All data are expressed as mean ± SD. **, $P < 0.005$, Student's t test.

activated in reserve ISCs, enabling their exit from quiescence. Upon Msi ablation, these cells can no longer enter the cell cycle, and the activity of CBCs (which do not require Msi activity) masks any phenotypic consequences of failed reserve ISC activation. Only upon radiation injury and CBC ablation do the phenotypic consequences of Msi loss and failed reserve ISC activation manifest themselves as failed epithelial regeneration.

If this model were correct, we would predict that premature exit of reserve ISCs from G0 and into the cell cycle should sensitize these cells and the intestinal epithelium to radiation damage, resulting in failed regeneration. To test this prediction, we drove reserve ISCs from G0 with a 24-h pulse of ectopic Msi1 induction in *TRE-Msi1* mice followed by exposure to 12 Gy γ-IR injury and quantified the frequency of clonal regenerative crypt foci. Indeed, in this context, the regenerative capacity of the epithelium was severely compromised (Fig. 6 A), providing support to the notion that maintenance of a pool of reserve ISCs in G0 acts as a protective mechanism for the tissue in the event of DNA damage. In contrast, doxycycline administration and Msi induction 48 h after γ-IR had no deleterious effects on regeneration of *TRE-Msi1* mice (Fig. S5 B).

Discussion

It is becoming increasingly clear that several tissues in adult mammals, most notably the hematopoietic system, bifurcate their stem cell compartments into a slow-cycling, quiescent stem cell capable of giving rise to a cycling, active stem cell (Li and Clevers, 2010). The benefit of such an organizational

structure is the capacity to promote tissue regeneration after damage while maintaining the proliferative output necessary to keep up with the demands of high-turnover tissues using a relatively small stem cell pool.

In the intestinal epithelium, recent studies have begun to define a hierarchical stem cell organization similar to that observed in the hematopoietic system, with a radioresistant, slow-cycling reserve ISC giving rise to an actively proliferating crypt base columnar cell, whose self-renewal is driven by high Wnt pathway activity (Li and Clevers, 2010; Montgomery et al., 2011; Takeda et al., 2011; Tian et al., 2011; Li et al., 2014; Asfaha et al., 2015). There has been considerable interest in gaining a better understanding of radioresistant intestinal cells that contribute to regeneration after damage by radiation/chemotherapy because of the relevance in the context of traditional cancer therapies, and also because of the apparent parallels between regeneration after damage and intestinal oncogenic transformation.

Recently, we have demonstrated that the Msi2 RNA-binding protein is capable of driving long-term hematopoietic stem cells out of quiescence and into the cell cycle (Kharas et al., 2010). In the intestinal epithelium, Msi1 and Msi2 function redundantly by binding to several transcripts that encode known negative regulators of mTORC1, including Pten, Bmpr1a, and Lrig1, and aberrant Msi activation leads to Pten repression and induction of the AKT–mTORC1 axis (Li et al., 2015; Wang et al., 2015).

In the current study, we investigated the function of the Msi family of RNA-binding proteins in intestinal stem cell function under basal conditions and during regeneration in response to injury. The data demonstrate that Msi1 and Msi2 are upregulated during the exit of reserve ISCs from quiescence, both under basal conditions and during regeneration after ablation of Wnt^{high} CBCs in response to high-dose radiation (Fig. 6 B). We therefore tested the sufficiency and necessity of Msi proteins for reserve stem cell activation and CBC self-renewal. Remarkably, genetic ablation of either *Msi* family member, as well as concomitant ablation of both *Msi1* and *Msi2* throughout the intestinal epithelium and colon, had no adverse effects on homeostasis, active CBC self-renewal, or Wnt pathway target gene expression, despite the high level of both Msi family members in the Wnt^{high} CBC stem cells (Potten et al., 2003; Cambuli et al., 2013; Li et al., 2015; Wang et al., 2015).

In contrast to the lack of phenotype in CBCs, *Msi* loss in of reserve ISCs (marked by either *Hopx-CreER* or *Bmi1-CreER)* resulted in the failure of these cells to become activated and contribute progeny to the epithelium. This failure of reserve ISC activation had no apparent detrimental consequences for the epithelium in the basal state, at least in the time period we investigated, likely because the unaffected CBC compartment provided the proliferative output necessary for epithelial maintenance. However, when mice lacking Msi activity in the entire epithelium or specifically in the very rare reserve ISCs were exposed to DNA-damaging γ-IR injury at levels known to ablate the CBC compartment, intestinal regeneration failed. This finding highlights the importance of these rare reserve ISCs in mounting a regenerative response in the face of injury.

When considering how reserve ISCs resist DNA damage, we analyzed their cell cycle status. Reserve ISCs are often referred to as being quiescent or residing in G0, as this state is thought of as being protective to stem cells in unfavorable environments (Cheung and Rando, 2013). Indeed, we observed that the majority of ISCs marked by *Hopx-CreER* or *Bmi1-CreER* reside in G0, whereas the remainder of the population cycles actively. We demonstrate that Msi activity controls the exit of reserve ISCs from the G0 state and their subsequent entry into the cell cycle. The importance of maintaining a pool of quiescent stem cells as a means to respond to injury can be observed in gain-of-function experiments in which ectopic activation of Msi1 drives reserve ISCs from quiescence. In this context, premature exit of this population from G0 and into the cell cycle renders the epithelium susceptible to radiation injury, supporting the notion that residence in G0 protects ISCs from DNA damage.

Interestingly, the phenotype of Msi loss of function is reminiscent of inactivation of mTORC1: both result in failed intestinal regeneration after injury and in G1 cell cycle arrest (Ashton et al., 2010; Kalaitzidis et al., 2012; Faller et al., 2015). We have previously established that in the context of colorectal cancer, mTORC1 is a functionally important target of Msi activity, and both mTORC1 and Msi are required for transformation of the epithelium downstream of APC loss. Consistent with our current findings, a recent study found that the negative regulator of mTORC1 activity, Pten, regulates the proliferation of intestinal stem cells marked with proxy reporter alleles driven by the mTert promoter (a population that likely overlaps with the *Hopx-/Bmi1-CreER*-marked population in the current study based on their functional and molecular similarities; Richmond et al., 2015). These findings are entirely consistent with observations in hematopoietic and muscle tissues that the mTORC1 complex similarly governs stem cell quiescence (Kalaitzidis et al., 2012; Rodgers et al., 2014).

Collectively, our findings emphasize the significance of tight regulation of reserve stem cell quiescence in protecting the intestinal epithelium from genotoxic insults. The discovery that Msi proteins govern reserve intestinal stem cell activation provides a foundation for future studies aimed at the development of therapeutic interventions that delay ISC cell cycle entry in an effort to protect patients against acute side effects of radiation therapy and radiation-induced acute gastrointestinal syndrome.

Materials and methods

Mouse strains

Lgr5-EGFP-IRES-CreER (JAX strain 008875), *Bmi1-CreER* (JAX strain 010531), and *R26-CAG-LSL-tdTomato* (JAX strain 007914) mice were obtained from The Jackson Laboratory. *Hopx-CreER* (JAX strain 017606) mice were generated at the University of Pennsylvania in the laboratory of J. Epstein (Philadelphia, PA). Mice were maintained on a C57/BL6N background.

Generation of the *TRE-Msi1* doxycycline-inducible mouse model and Msi1 and Msi2 conditional alleles was previously described (Li et al., 2015; Park et al., 2015). They were crossed with mice harboring tamoxifen-inducible Cre recombinases (*Villin-*, *Hopx-*, *Bmi1-*, and *Lgr5-CreER* mice) for conditional deletion of floxed alleles or activation of fluorescent reporter (el Marjou et al., 2004; Barker et al., 2007; Sangiorgi and Capecchi, 2008; Takeda et al., 2011).

All experimental analyses were performed on three or more individual mice (male or female mice at 8–12 wk of age). Controls and experimental groups were either sex-matched littermates or age-matched, sex-matched nonlittermates. To ablate *Msi* genes or activate the *R26-LSL-tdTomato* reporter, tamoxifen (Sigma-Aldrich) was dissolved in corn oil at 10 mg/ml, and 1 mg tamoxifen was injected

intraperitoneally for each dose. To induce *Msi1* gene expression, *TRE-Msi1* and control (*M2rtTA* alone) mice received 1 mg/ml doxycycline hyclate (Sigma-Aldrich) in drinking water, supplemented with 1% (wt/vol) sucrose. 12 Gy whole-body γ-IR was administered to at least three mice in each group. All mouse protocols were approved by the Institutional Animal Care and Use Committee at the University of Pennsylvania under protocol 803415 (C.J. Lengner).

Histology, immunofluorescence, and immunochemistry

Tissues were fixed in 4% PFA overnight at 4°C, washed in PBS, and moved to 70% ethanol before paraffin embedding and sectioning. Hematoxylin, eosin, Alcian blue, and alkaline phosphatase staining was performed according to standard procedures in the Morphology Core of the Penn Center for Molecular Studies in Digestive and Liver Diseases. For immunostaining, antigen retrieval was performed by heating slides in 10 mM citrate buffer (10 mM sodium citrate and 0.05% Tween 20, pH 6) or Tris/EDTA buffer (10 mM Tris base, 1 mM EDTA solution, and 0.05% Tween 20, pH 9) with a pressure cooker.

Leica Biosystems SP5 (LAS AF software) and SP8 confocal microscopes (LAS X software) were used for fluorescence microscopy equipped with 10× dry, 20× dry, 40× water, and 63× oil objectives. An E600 microscope (Nikon) equipped with 10×, 20×, and 40× bright-field objectives (iVision software) was used for light microscopy. Imaging was performed at RT.

The following primary antibodies were used for immunostaining: Living Colors DsRed polyclonal antibody (1:200, 632496; Takara Bio Inc.), anti-Ki67 antibody (1:1,000, NCL-Ki67p; Leica Biosystems), anti-Musashi1 antibody (1:200, D270-3; MBL International), anti-Musashi2 antibody (1:200, NBP1-42029; Novus Biologicals), anti–β-catenin antibody (1:1,000, C7207; Sigma-Aldrich), anti–E-cadherin (1:200, 13-1900; Invitrogen), and anti–lysozyme C antibody (C-19, 1:200, sc-27958; Santa Cruz Biotechnology, Inc.). Cy2-, Cy3-, and Cy5-conjugated secondary antibodies were obtained from Jackson ImmunoResearch Laboratories, Inc. Biotinylated secondary antibodies and DAB substrate kit for immunohistochemistry were purchased from Vector Laboratories.

All quantifications were done on 20–40 randomly selected areas in proximal or distal intestine of at least three mice in each group. For quantification of regenerative efficiency, surviving crypts were defined as 10 or more adjacent chromophilic cells and a lumen in hematoxylin and eosin–stained sections from intestinal epithelium.

For quantification of Msi1 fluorescence intensity, tdTomato$^+$ populations were sorted by FACS from experimental and control mice, smeared over coverslips coated with CELL-TAK (354240; Corning), and allowed to settle at 37°C for 10 min. The cells were subsequently fixed in 4% PFA and permeabilized in 0.5% Triton X-100 before staining. Quantification of fluorescence intensity was done using MetaMorph Microscopy Automation and Image Analysis Software.

Intestinal epithelial cell isolation

Intestinal epithelial cells were isolated as described previously (Sato et al., 2009), with modifications. Small intestine was dissected out of mice of the appropriate genotype, opened longitudinally, and washed twice with cold PBS. The tissue was incubated in 5 mM EDTA/HBSS for 10 min at 4°C, and the villi were gently scraped off using a glass coverslip. The intestine was minced, placed into fresh 5 mM EDTA/HBSS, and incubated for 30 min on ice. After transfer of tissue into fresh EDTA/HBSS buffer, the tissue fragments were vigorously suspended by pipetting. The supernatant was centrifuged at 1,500 rpm for 5 min to collect crypts.

Flow cytometry

For flow cytometry analysis, a single-cell suspension was made by incubation of isolated crypts or total epithelium in 0.05% trypsin for 10 min at RT. Lgr5$^+$ stem cells were quantified by flow cytometry on cells isolated from *Lgr5-eGFP-IRES-CreER*. Frequency of *Bmi1-Tomato* and *Hopx-Tomato* ISCs were quantified by flow cytometry on cells isolated from *Bmi1-CreER::Lox-Stop-Lox-tdTomato* and *Hopx-CreER::Lox-Stop-Lox-tdTomato* 18 h after tamoxifen injection. 1 µg/ml DAPI was used to exclude dead cells from the quantification of ISCs. For quiescence (G0) analysis, tdTomato$^+$ cells were sorted by FACS from experimental and control mice into 100% ethanol and placed at 4°C overnight. The cells were then stained with pyronin Y (1 µg/ml) and DAPI (10 µg/ml) for 30 min before flow cytometric analysis. EdU incorporation was assessed by intraperitoneal injection of mice with 30 mg/kg EdU 2–4 h before tissue harvest, and incorporation was analyzed with Click-it EdU assay kit (C10634; Thermo Fisher Scientific) and flow cytometry.

Quantitative RT-PCR

1 µg total RNA was used in a 20-µl first-strand cDNA synthesis reaction (Thermo Fisher Scientific). SYBR green quantitative RT-PCR was performed under standard conditions using a QuantStudio 6 Flex (Thermo Fisher Scientific), and data were analyzed using QuantStudio RT-PCR software. Custom primers were validated with standard SYBR green qRT-PCR. Data were normalized to housekeeping gene *Gapdh*. The following sets of primers were used to assess Msi1 and Msi mRNA expression levels: Msi1, 5′-GCCATG CTGATGTTCGACAA-3′ and 5′-CTACGATGTCCTCGCTCT CAA-3′; Msi2, 5′-GCGATGCTGATGTTCGACAA-3′ and 5′-TCT CCACAACGTCTTCATTCTCA-3′.

Determination of recombination of Msi1 and Msi2 genes:

DNA was extracted from eGFP$^+$ dtTomato$^+$ sorted cells from *Msi1$^{flx/flx}$::Msi2$^{flx/flx}$::Lgr5-EGFP-IRES-CreER::LSl-tdTomato* mice. DNA was resuspended in Tris/EDTA, and the concentration was normalized before PCR. The following sets of forward and reverse primers were used: Msi1 floxed and wild-type, 5′-CGGACTGGGAGAGGTTTCTT-3′ and 5′-AGCTCCCCTGATTCCTGGT-3′; Msi2 floxed and wild-type, 5′-GCTCGGCTGACAAAGAAAGT-3′ and 5′-TCTCCTTGTTGCGCT CAGTA-3′; Msi2 null, 5′-CCTGTCTGGTTGCTTCCTCG-3′ and 5′-GAGCCAACTCGCTAGCTTG-3′. These primers were used to detect wild-type, floxed, and null alleles using Hot Start DNA polymerase (CB4040; Denville Scientific).

Organoid culture

50 isolated crypts were mixed with 50 µl Matrigel (BD) and plated in 24-well plates. After polymerization of Matrigel, 500 µl crypt culture medium (advanced DMEM/F12 containing 50 ng/ml EGF [Invitrogen], 0.5 µg/ml R-spondin 1 [The Wistar Institute], 100 ng/ml Noggin [PeproTech], and 3 µM GSK-3 inhibitor [CHIR99021; Stemgent]) was added. In Fig. 1 E, the culture medium contains no CHIR99021 and 0–0.5 µg/ml R-spondin 1.

Fluidigm single-cell gene expression

For the single-cell gene expression graphs in Fig. 3 B, raw data were extracted from Li et al. (2014). Full methodology is provided in that reference as well. Raw data for Fig. 5 (E and F) and Fig. S5 are provided in Table S2.

Transcriptome profiling

Total RNA was isolated from crypts of mouse small intestinal epithelium cells from three control and three *Msi-DKO* mice that received five doses of tamoxifen (1 mg each dose, T5648-1G; Sigma-Aldrich)

for five consecutive days 1 wk before tissue harvest. Total RNA was isolated using TRIzol Reagent (Thermo Fisher Scientific) according to the manufacturer's instructions. Total RNA was DNase treated with an RNase-free DNase kit (Zymo Research). Purified RNA was submitted to the University of Pennsylvania Molecular Profiling Core, where samples were labeled and hybridized to Affymetrix Mouse Gene 1.0ST arrays. Microarray data were analyzed using Partek Genomics Suite software. After RMA background subtraction and normalization, one-way analysis of variance between controls and *Msi-DKO* was run to compute p-values of significance and *F* statistic for each probe set. The *q* value, a measure of false discovery rate (FDR), was computed within the significance analysis of microarrays software for each probe set by running an unpaired *t* test. The FDR values were integrated with the one-way analysis of variance results. The set of differentially expressed genes were selected as those that were significant at an FDR cutoff of 5% and a p-value of 0.05 and that changed at least 1.5-fold in either direction in the *Msi-DKO* group compared with the control group.

Statistical analysis

Throughout all figures, center values represent means. We performed unpaired Student's *t* tests to calculate p-values. Error bars reflect SD. For animal studies, samples were excluded from experiments if animals were considered unhealthy.

Online supplemental material

Figs. S1 and S2 show that Msi loss does not affect proliferation and differentiation of epithelial cells and CBCs in the intestine and colon under basal conditions. Fig. S3 shows that Msi loss impairs regeneration in *Msi* knockout mice after high-dose irradiation. Fig. S4 shows Msi up-regulation in regenerative crypt foci after radiation injury. Fig. S5 shows that Msi up-regulation activates metabolic genes. Table S1 lists gene expression values in *Msi DKO* and control intestinal crypts. Table S2 shows raw data for single-cell gene expression profiling of *Lgr5*$^+$ CBCs and *Bmi1-CreER*$^+$ reserve ISCs.

Acknowledgments

We thank John Tobias at the Penn Genomic Analysis Core for assistance with analysis of transcriptome profiling data.

M. Yousefi is a Howard Hughes Medical Institute International Student Research fellow (59107993). M.G. Kharas was supported by the U.S. National Institutes of Health National Institute of Diabetes and Digestive and Kidney Diseases Career Development Award, National Institute of Diabetes and Digestive and Kidney Diseases (R01-DK101989-01A1), National Cancer Institute (1R01CA193842-01), Louis V. Gerstner Young Investigator Award, and the American Society of Hematology Junior Scholar Award, Kimmel Scholar Award, V-Scholar Award, and Geoffrey Beene Award. C.J. Lengner was supported by a grant from the Pennsylvania Department of Health (Health Research Formula Fund #4100054874), National Institute of Diabetes and Digestive and Kidney Diseases (R01 DK106309), and National Cancer Institute (R01 CA168654). This work was supported in part by the National Institutes of Health/National Institute of Diabetes and Digestive and Kidney Diseases Center for Molecular Studies in Digestive and Liver Diseases (P30DK050306) and its core facilities.

The authors declare no competing financial interests.

Submitted: 27 April 2016
Revised: 12 August 2016
Accepted: 29 September 2016

References

Asfaha, S., Y. Hayakawa, A. Muley, S. Stokes, T.A. Graham, R.E. Ericksen, C.B. Westphalen, J. von Burstin, T.L. Mastracci, D.L. Worthley, et al. 2015. Krt19(+)/Lgr5(-) cells are radioresistant cancer-initiating stem cells in the colon and intestine. *Cell Stem Cell.* 16:627–638. http://dx.doi.org/10.1016/j.stem.2015.04.013

Ashton, G.H., J.P. Morton, K. Myant, T.J. Phesse, R.A. Ridgway, V. Marsh, J.A. Wilkins, D. Athineos, V. Muncan, R. Kemp, et al. 2010. Focal adhesion kinase is required for intestinal regeneration and tumorigenesis downstream of Wnt/c-Myc signaling. *Dev. Cell.* 19:259–269. http://dx.doi.org/10.1016/j.devcel.2010.07.015

Barker, N., J.H. van Es, J. Kuipers, P. Kujala, M. van den Born, M. Cozijnsen, A. Haegebarth, J. Korving, H. Begthel, P.J. Peters, and H. Clevers. 2007. Identification of stem cells in small intestine and colon by marker gene Lgr5. *Nature.* 449:1003–1007. http://dx.doi.org/10.1038/nature06196

Cambuli, F.M., A. Rezza, J. Nadjar, and M. Plateroti. 2013. Musashi1-eGFP mice, a new tool for differential isolation of the intestinal stem cell populations. *Stem Cells.* 31:2273–2278. http://dx.doi.org/10.1002/stem.1428

Cambuli, F.M., B.R. Correa, A. Rezza, S.C. Burns, M. Qiao, P.J. Uren, E. Kress, A. Boussouar, P.A. Galante, L.O. Penalva, and M. Plateroti. 2015. A mouse model of targeted Musashi1 expression in whole intestinal epithelium suggests regulatory roles in cell cycle and stemness. *Stem Cells.* 33:3621–3634. http://dx.doi.org/10.1002/stem.2202

Ch'ang, H.J., J.G. Maj, F. Paris, H.R. Xing, J. Zhang, J.P. Truman, C. Cardon-Cardo, A. Haimovitz-Friedman, R. Kolesnick, and Z. Fuks. 2005. ATM regulates target switching to escalating doses of radiation in the intestines. *Nat. Med.* 11:484–490. http://dx.doi.org/10.1038/nm1237

Cheng, H., and C.P. Leblond. 1974. Origin, differentiation and renewal of the four main epithelial cell types in the mouse small intestine. V. Unitarian theory of the origin of the four epithelial cell types. *Am. J. Anat.* 141:537–561. http://dx.doi.org/10.1002/aja.1001410407

Cheung, T.H., and T.A. Rando. 2013. Molecular regulation of stem cell quiescence. *Nat. Rev. Mol. Cell Biol.* 14:329–340. http://dx.doi.org/10.1038/nrm3591

el Marjou, F., K.P. Janssen, B.H. Chang, M. Li, V. Hindie, L. Chan, D. Louvard, P. Chambon, D. Metzger, and S. Robine. 2004. Tissue-specific and inducible Cre-mediated recombination in the gut epithelium. *Genesis.* 39:186–193. http://dx.doi.org/10.1002/gene.20042

Faller, W.J., T.J. Jackson, J.R. Knight, R.A. Ridgway, T. Jamieson, S.A. Karim, C. Jones, S. Radulescu, D.J. Huels, K.B. Myant, et al. 2015. mTORC1-mediated translational elongation limits intestinal tumour initiation and growth. *Nature.* 517:497–500. http://dx.doi.org/10.1038/nature13896

Fukada, S., A. Uezumi, M. Ikemoto, S. Masuda, M. Segawa, N. Tanimura, H. Yamamoto, Y. Miyagoe-Suzuki, and S. Takeda. 2007. Molecular signature of quiescent satellite cells in adult skeletal muscle. *Stem Cells.* 25:2448–2459. http://dx.doi.org/10.1634/stemcells.2007-0019

Hope, K.J., S. Cellot, S.B. Ting, T. MacRae, N. Mayotte, N.N. Iscove, and G. Sauvageau. 2010. An RNAi screen identifies Msi2 and Prox1 as having opposite roles in the regulation of hematopoietic stem cell activity. *Cell Stem Cell.* 7:101–113. http://dx.doi.org/10.1016/j.stem.2010.06.007

Hua, G., T.H. Thin, R. Feldman, A. Haimovitz-Friedman, H. Clevers, Z. Fuks, and R. Kolesnick. 2012. Crypt base columnar stem cells in small intestines of mice are radioresistant. *Gastroenterology.* 143:1266–1276. http://dx.doi.org/10.1053/j.gastro.2012.07.106

Hüttmann, A., S.L. Liu, A.W. Boyd, and C.L. Li. 2001. Functional heterogeneity within rhodamine123(lo) Hoechst33342(lo/sp) primitive hemopoietic stem cells revealed by pyronin Y. *Exp. Hematol.* 29:1109–1116. http://dx.doi.org/10.1016/S0301-472X(01)00684-1

Ito, T., H.Y. Kwon, B. Zimdahl, K.L. Congdon, J. Blum, W.E. Lento, C. Zhao, A. Lagoo, G. Gerrard, L. Foroni, et al. 2010. Regulation of myeloid leukaemia by the cell-fate determinant Musashi. *Nature.* 466:765–768. http://dx.doi.org/10.1038/nature09171

Itzkovitz, S., A. Lyubimova, I.C. Blat, M. Maynard, J. van Es, J. Lees, T. Jacks, H. Clevers, and A. van Oudenaarden. 2011. Single-molecule transcript counting of stem-cell markers in the mouse intestine. *Nat. Cell Biol.* 14:106–114. http://dx.doi.org/10.1038/ncb2384

Kalaitzidis, D., S.M. Sykes, Z. Wang, N. Punt, Y. Tang, C. Ragu, A.U. Sinha, S.W. Lane, A.L. Souza, C.B. Clish, et al. 2012. mTOR complex 1 plays critical roles in hematopoiesis and Pten-loss-evoked leukemogenesis. *Cell Stem Cell.* 11:429–439. http://dx.doi.org/10.1016/j.stem.2012.06.009

Katz, Y., F. Li, N.J. Lambert, E.S. Sokol, W.L. Tam, A.W. Cheng, E.M. Airoldi, C.J. Lengner, P.B. Gupta, Z. Yu, et al. 2014. Musashi proteins are post-transcriptional regulators of the epithelial-luminal cell state. *eLife.* 3:e03915. http://dx.doi.org/10.7554/eLife.03915

Kharas, M.G., C.J. Lengner, F. Al-Shahrour, L. Bullinger, B. Ball, S. Zaidi, K. Morgan, W. Tam, M. Paktinat, R. Okabe, et al. 2010. Musashi-2 regulates normal hematopoiesis and promotes aggressive myeloid leukemia. *Nat. Med.* 16:903–908. http://dx.doi.org/10.1038/nm.2187

Li, L., and H. Clevers. 2010. Coexistence of quiescent and active adult stem cells in mammals. *Science.* 327:542–545. http://dx.doi.org/10.1126/science.1180794

Li, N., M. Yousefi, A. Nakauka-Ddamba, R. Jain, J. Tobias, J.A. Epstein, S.T. Jensen, and C.J. Lengner. 2014. Single-cell analysis of proxy reporter allele-marked epithelial cells establishes intestinal stem cell hierarchy. *Stem Cell Rep.* 3:876–891. http://dx.doi.org/10.1016/j.stemcr.2014.09.011

Li, N., M. Yousefi, A. Nakauka-Ddamba, F. Li, L. Vandivier, K. Parada, D.H. Woo, S. Wang, A.S. Naqvi, S. Rao, et al. 2015. The Msi family of RNA-binding proteins function redundantly as intestinal oncoproteins. *Cell Reports.* 13:2440–2455. http://dx.doi.org/10.1016/j.celrep.2015.11.022

Li, N., A. Nakauka-Ddamba, J. Tobias, S.T. Jensen, and C.J. Lengner. 2016. Mouse label-retaining cells are molecularly and functionally distinct from reserve intestinal stem cells. *Gastroenterology.* 151:298–310.e7. http://dx.doi.org/10.1053/j.gastro.2016.04.049

Metcalfe, C., N.M. Kljavin, R. Ybarra, and F.J. de Sauvage. 2014. Lgr5+ stem cells are indispensable for radiation-induced intestinal regeneration. *Cell Stem Cell.* 14:149–159. http://dx.doi.org/10.1016/j.stem.2013.11.008

Montgomery, R.K., D.L. Carlone, C.A. Richmond, L. Farilla, M.E. Kranendonk, D.E. Henderson, N.Y. Baffour-Awuah, D.M. Ambruzs, L.K. Fogli, S. Algra, and D.T. Breault. 2011. Mouse telomerase reverse transcriptase (mTert) expression marks slowly cycling intestinal stem cells. *Proc. Natl. Acad. Sci. USA.* 108:179–184. http://dx.doi.org/10.1073/pnas.1013004108

Park, S.M., R.P. Deering, Y. Lu, P. Tivnan, S. Lianoglou, F. Al-Shahrour, B.L. Ebert, N. Hacohen, C. Leslie, G.Q. Daley, et al. 2014. Musashi-2 controls cell fate, lineage bias, and TGF-β signaling in HSCs. *J. Exp. Med.* 211:71–87. http://dx.doi.org/10.1084/jem.20130736

Park, S.M., M. Gönen, L. Vu, G. Minuesa, P. Tivnan, T.S. Barlowe, J. Taggart, Y. Lu, R.P. Deering, N. Hacohen, et al. 2015. Musashi2 sustains the mixed-lineage leukemia-driven stem cell regulatory program. *J. Clin. Invest.* 125:1286–1298. http://dx.doi.org/10.1172/JCI78440

Pazhanisamy, S.K. 2009. Stem cells, DNA damage, ageing and cancer. *Hematol. Oncol. Stem Cell Ther.* 2:375–384. http://dx.doi.org/10.1016/S1658-3876(09)50005-2

Potten, C.S. 2004. Radiation, the ideal cytotoxic agent for studying the cell biology of tissues such as the small intestine. *Radiat. Res.* 161:123–136. http://dx.doi.org/10.1667/RR3104

Potten, C.S., C. Booth, G.L. Tudor, D. Booth, G. Brady, P. Hurley, G. Ashton, R. Clarke, S. Sakakibara, and H. Okano. 2003. Identification of a putative intestinal stem cell and early lineage marker; musashi-1. *Differentiation.* 71:28–41. http://dx.doi.org/10.1046/j.1432-0436.2003.700603.x

Rezza, A., S. Skah, C. Roche, J. Nadjar, J. Samarut, and M. Plateroti. 2010. The overexpression of the putative gut stem cell marker Musashi-1 induces tumorigenesis through Wnt and Notch activation. *J. Cell Sci.* 123:3256–3265. http://dx.doi.org/10.1242/jcs.065284

Richmond, C.A., M.S. Shah, L.T. Deary, D.C. Trotier, H. Thomas, D.M. Ambruzs, L. Jiang, B.B. Whiles, H.D. Rickner, R.K. Montgomery, et al. 2015. Dormant intestinal stem cells are regulated by PTEN and nutritional status. *Cell Reports.* 13:2403–2411. http://dx.doi.org/10.1016/j.celrep.2015.11.035

Rodgers, J.T., K.Y. King, J.O. Brett, M.J. Cromie, G.W. Charville, K.K. Maguire, C. Brunson, N. Mastey, L. Liu, C.R. Tsai, et al. 2014. mTORC1 controls the adaptive transition of quiescent stem cells from G0 to G(Alert). *Nature.* 510:393–396. http://dx.doi.org/10.1038/nature13255

Sakakibara, S., Y. Nakamura, T. Yoshida, S. Shibata, M. Koike, H. Takano, S. Ueda, Y. Uchiyama, T. Noda, and H. Okano. 2002. RNA-binding protein Musashi family: Roles for CNS stem cells and a subpopulation of ependymal cells revealed by targeted disruption and antisense ablation. *Proc. Natl. Acad. Sci. USA.* 99:15194–15199. http://dx.doi.org/10.1073/pnas.232087499

Sangiorgi, E., and M.R. Capecchi. 2008. Bmi1 is expressed in vivo in intestinal stem cells. *Nat. Genet.* 40:915–920. http://dx.doi.org/10.1038/ng.165

Sato, T., R.G. Vries, H.J. Snippert, M. van de Wetering, N. Barker, D.E. Stange, J.H. van Es, A. Abo, P. Kujala, P.J. Peters, and H. Clevers. 2009. Single Lgr5 stem cells build crypt-villus structures in vitro without a mesenchymal niche. *Nature.* 459:262–265. http://dx.doi.org/10.1038/nature07935

Spears, E., and K.L. Neufeld. 2011. Novel double-negative feedback loop between adenomatous polyposis coli and Musashi1 in colon epithelia. *J. Biol. Chem.* 286:4946–4950. http://dx.doi.org/10.1074/jbc.C110.205922

Takeda, N., R. Jain, M.R. LeBoeuf, Q. Wang, M.M. Lu, and J.A. Epstein. 2011. Interconversion between intestinal stem cell populations in distinct niches. *Science.* 334:1420–1424. http://dx.doi.org/10.1126/science.1213214

Tao, S., D. Tang, Y. Morita, T. Sperka, O. Omrani, A. Lechel, V. Sakk, J. Kraus, H.A. Kestler, M. Kühl, and K.L. Rudolph. 2015. Wnt activity and basal niche position sensitize intestinal stem and progenitor cells to DNA damage. *EMBO J.* 34:624–640. http://dx.doi.org/10.15252/embj.201490700

Tetteh, P.W., O. Basak, H.F. Farin, K. Wiebrands, K. Kretzschmar, H. Begthel, M. van den Born, J. Korving, F. de Sauvage, J.H. van Es, et al. 2016. Replacement of lost Lgr5-positive stem cells through plasticity of their enterocyte-lineage daughters. *Cell Stem Cell.* 18:203–213. http://dx.doi.org/10.1016/j.stem.2016.01.001

Tian, H., B. Biehs, S. Warming, K.G. Leong, L. Rangell, O.D. Klein, and F.J. de Sauvage. 2011. A reserve stem cell population in small intestine renders Lgr5-positive cells dispensable. *Nature.* 478:255–259. http://dx.doi.org/10.1038/nature10408

Wang, S., N. Li, M. Yousefi, A. Nakauka-Ddamba, F. Li, K. Parada, S. Rao, G. Minuesa, Y. Katz, B.D. Gregory, et al. 2015. Transformation of the intestinal epithelium by the MSI2 RNA-binding protein. *Nat. Commun.* 6:6517. http://dx.doi.org/10.1038/ncomms7517

Yan, K.S., L.A. Chia, X. Li, A. Ootani, J. Su, J.Y. Lee, N. Su, Y. Luo, S.C. Heilshorn, M.R. Amieva, et al. 2012. The intestinal stem cell markers Bmi1 and Lgr5 identify two functionally distinct populations. *Proc. Natl. Acad. Sci. USA.* 109:466–471. http://dx.doi.org/10.1073/pnas.1118857109